Sugarcane Bagasse Ash as a Reinforcing Filler in Thermoplastic Elastomers: Structural and Mechanical Characterizations

Maiza da Silva Ozório, Elton Aparecido Prado dos Reis, Silvio Rainho Teixeira, Felipe Silva Bellucci, Aldo Eloizo Job

Laboratório de Tecnologia de Borrachas e Aplicações, Departamento de Física, Química e Biologia, Universidade Estadual Paulista – FCT/UNESP, Presidente Prudente – SP, CEP: 19060-900, Sao Paulo, Brazil
Correspondence to: A. Job (E-mail: job@fct.unesp.br)

ABSTRACT: The incorporation of residues as reinforcing fillers in polymer composites has emerged as a viable solution, enabling improvements in the mechanical properties of these materials, and has also resulted in a reduction in the cost of the final product. In this work, sugarcane bagasse ash (SBA) was used as a reinforcing filler in comparison with commercial silica (CS) in thermoplastic elastomers prepared from the compatibility of low-density polyethylene (LDPE) with natural rubber (NR). The composites were obtained by a physical mixture of LDPE and NR with different proportions of CS and SBA using a Haake rotational rheometer. The samples were analyzed by Raman spectroscopy, Fourier transform infrared spectroscopy (FTIR), scanning electron microscopy (SEM), and tensile testing. The results show that SBA has similar properties to CS, thus making its use feasible as a reinforcing filler in thermoplastic elastomers. © 2014 Wiley Periodicals, Inc. J. Appl. Polym. Sci. **2015**, *132*, 41466.

INTRODUCTION

The main fillers used to improve the mechanical properties of polymeric composites are vegetable fibers and their derivatives, glass fibers, carbon black and oxide particles, such as silica (SiO_2) and alumina (Al_2O_3).[1,2] The choice of load is a very important and critical point because, in addition to having a great impact on the final properties of the material, it is also of great importance in determining the cost of the product.[3] Thus, the characteristics of the composites depend on the properties of the components, such as interaction and synergy between constituent materials, porosity of fillers, dispersion and quantity of the fillers, and so on.[4,5]

Environmental preservation needs to drive industry toward waste recycling. In this sense, the use of solid waste as a reinforcing filler has been the focus of many research groups because of its great potential to replace traditional load materials.[6,7] Solid residue is the term used to designate the solid waste resulting from industries, hospitals, businesses, agriculture, and similar segments. If these materials are disposed of incorrectly, they can cause serious health and environmental problems. One way to reduce the impact of these materials on the environment is giving them an application which can be used as a way of adding to their economic value.[8]

In Brazil, there is a kind of residue named bagasse that deserves special attention because it is generated in large quantities. The generation of bagasse is associated with the high demand for sugarcane used in the production of ethanol and sugar.[9,10] In general, sugarcane bagasse is burned in sugarcane factories, in boilers through a system known as energy cogeneration, which is the production of steam supplying mechanical turbines and for the production of electricity.[11] The burning of sugarcane bagasse generates another residue called Sugarcane Bagasse Ash (SBA), and for each ton of bagasse burned, approximately 25 kg of ash are generated.[12] This ash has no favorable, common applications and, although it is not directly released in the air, it pollutes the environment when disposed of improperly.

In view of the perspectives for the growth of the sugarcane industry and the desire to promote sustainable development in Brazil, a large number of studies have been carried out in order to find a new destination for the ash from burned sugarcane bagasse. These studies show that the SBA is mainly composed of silica (SiO_2).[6] The silica is absorbed from the earth by the roots of cane sugar in the form of silicic acid (H_4SiO_4) which is almost entirely transported to the leaves.

The emergence of various stages of silica (amorphous or crystalline) depends on the temperature at which the bagasse is

Table I. Lists of the Chemical Elements Contained in the SBA Determined by X-ray Fluorescence Spectroscopy

Material	Chemical elements				
SBA	Si	Al	Fe	Na	K
	85.5	5.3	1.3	–	3.5
	Ca	Mg	Mn	Ti	P
	2.1	1.1	0.1	0.3	0.5

burned, the presence of crystalline material being due to the high combustion temperatures in the boilers. In addition to the influence on the crystallinity degree of the silica, the burning conditions also influence the specific surface area of the particles. For ash obtained from controlled condition burning, the specific surface area is a function of the micropore volume. The microporosity and irregularities of the particles of SBA that confer high values of a specific surface area to them are related to the amount of carbon present in the ash.[13,14] For burning between 400°C and 500°C, the carbon, which is black in color, is maintained in the ash, as it is amorphous and combined with other elements.[15]

According to the characteristics exhibited by the SBA, it is possible to incorporate it as a filler in thermoplastic elastomers (TPE). The TPEs are one of the most exploited polymeric materials in scientific and technological areas,[16,17] and their applications depend on their properties, which are determined by the composition, the structure of the constituents, and the molecular structure.[18] Thus, the ultimate tensile strength in the TPEs can be improved by the incorporation of an elastomeric component (in the form of blend or copolymerization) or by adding a reinforcing filler to the polymer matrix, such as silica from the SBA.[19]

In this work, the thermoplastic elastomers (NR/LDPE) were prepared using natural rubber (NR) as an elastomeric constituent and low density polyethylene (LDPE) as a thermoplastic component. The sugarcane bagasse ash (SBA) and commercial silica (CS) were added to the thermoplastic elastomer in various concentrations in order to investigate the influence of SBA and CS on the structural, morphological and mechanical properties of the composite. The main aim of this work was the development of an innovative and sustainable composite using SBA instead of CS that can be used in various technological or industrial areas adding economic value to this waste (SBA) from sugarcane bagasse and, thus, creating a new option for utilization of the SBA.

MATERIALS AND METHODS

Materials for the Thermoplastic Elastomers NR/LDPE

Base Material. Dry natural rubber (NR) of the commercial variety CCB (*Crepe Claro Brasileiro*—CCB) financed by the *DLP Industria e Comércio de Borracha e Artefatos* [R] in the city of Poloni/SP and low density polyethylene (LDPE), supplied by the Valimplast® company located in Nova Santa Rita—RS were used for the preparation of the thermoplastic elastomers (NR/LDPE). This NR or cis-1,4-polyisoprene was obtained in processing plants by the coagulation of latex from the *Hevea brasiliensis* species, clones RRIM 600 while the LDPE is made from the polymeriza-

tion of ethylene, in general, in autoclave or tubular reactors at very high pressures. The base material of NR/LDPE was manufactured with a weight proportion of 50% LDPE and 50% NR.

Vulcanization Systems Without Sulphur. The vulcanization system used for the preparation of the thermoplastic elastomers (NR/LDPE) was based only on accelerator reagents, in this case, TMTD and CBC. Start reagents, chemical formula, purity and origin of the base formulation, vulcanization, and acceleration systems utilized were: zinc oxide (ZnO, 81.38 g/mol, analytical purity, VETEC), stearic acid ($CH_3(CH_2)_{16}COOH$, 284.48 g/mol, analytical purity, VETEC), N-Ciclohexil-2-benzotiazol-sulfenamide (CBC) ($C_{13}H_{16}N_2S_2$, 264.42 g/mol, analytical purity, Nord Chemie), and tetramethylthiuram disulfide (TMTD) ($[(CH_3)_2NCS_2]_2$, 240.43 g/mol, $\geq$ 94%, LANXESS Energizing Chemistry).

Commercial Silica (CS). The commercial silica utilized in this work was a precipitated synthetic amorphous silica, ZEOSIL 175, financed by the Solvay Silica Korea Co., Ltd, with a molecular weight of 60.2 g/mol, density equal to 2.1 g/cm^3 and purity equal to 95%.

Sugarcane Bagasse Ash (SBA). The SBA was fractionated (sieved) using sieves of 16, 32, 60, 115, and 270 meshes. The smaller size fraction, 270 meshes, was used for the production of composites. Table I lists the chemical elements contained in the SBA determined by X Ray Fluorescence Spectroscopy. The thermoplastic elastomers NR/LDPE and NR/LDPE with CS and SBA formulations are listed in Table II.

Preparation of the Thermoplastic Elastomers NR/LDPE

The processing of the natural rubber formulations was carried out in an open mixing mill or a rubber mixer (Haake rotational rheometer, model Polylab OS) for 20 min at 126°C and 80 Hz. The thermoplastic elastomers NR/LDPE were made with dry natural (50 phr), low-density polyethylene (50 phr), a

Table II. List of Components and Their Receptivity Quantities for the Thermoplastic Elastomers NR/LDPE and NR/LDPE with CS and SBA

Components	Quantity (phr[a])
Base formulation	
Dry natural rubber (NR)	50
Polyethylene (LDPE)	50
Vulcanization system	
Activators	
Zinc oxide	3
Stearic acid	2
Accelerators	
CBC[b]	1.2
TMTD[c]	2
Composites	
Proportion CS/SBA	10/0; 7.5/2.5; 5/5; 2.5/7.5; and 0/10

[a] phr: Parts per hundred of rubber.
[b] CBC: N-Ciclohexil-2-benzotiazol-sulfenamide.
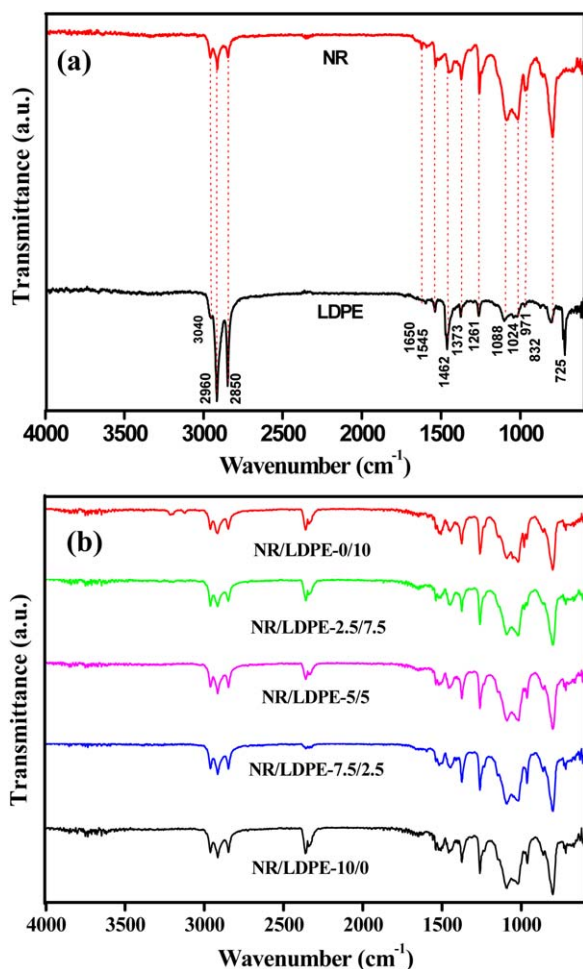[c] TMTD: Tetramethylthiuram Disulfide.

Figure 1. (a) Infrared spectra at room temperature of NR and LDPE and (b) of the thermoplastic elastomers NR/LDPE with different proportions of CS and SBA. In detail, the maximum frequency values for the main characteristic bands. [Color figure can be viewed in the online issue, which is available at wileyonlinelibrary.com.]

vulcanization system consisting of zinc oxide (3 phr) and stearic acid (3 phr), which reacted with each other to form zinc stearate $[2.(C_{17}H_{35}COOH) + ZnO \rightarrow (C_{17}H_{35}COO^-)_2.Zn^{2+} + H_2O]$ and an accelerating system consisting of CBC (1.2 phr) and TMTD (2 phr). Different proportions of CS and SBA (10/0; 7.5/2.5; 5/5; 2.5/7.5; and 0/10) were added to the thermoplastic elastomers NR/LDPE. All the quantities were mixed as noted in Table I. After undergoing the mixing process, the formulations were compression molded at 150°C with a closing pressure of 7.5 Ton in a pneumatic press for 3 min. This time parameter was previously obtained from rheological assays. At the end of process, the following samples of NR/LDPE-CS/SBA were prepared: NR/LDPE-0/0, NR/LDPE-10/0, NR/LDPE-7.5/2.5, NR/LDPE-5/5, NR/LDPE-2.5/7.5, and NR/LDPE-0/10. Similar techniques of processing have been reported.[20,21]

Structural Characterization

The structural characterization of the thermoplastic elastomers was carried out by Fourier Transform Infrared Spectroscopy (FTIR) and micro-Raman spectroscopy (Raman). The FTIR spectrophotometer used was a Bruker model Vector 22, in the region of 4,000–500 cm^{-1}, with an accuracy of 2 cm^{-1} and 128 scans. The Attenuated total reflectance (ATR) technique was used to examine the composite surface directly. The Raman spectrophotometer used was a Renishaw model In-Via, a laser with a wavelength equal to 663 nm and power of 50 mW.

Morphological Characterization

The morphological characterization of the composites was studied using a Carls Zeiss scanning electron microscope (SEM), model EVO LS15, and a secondary electron detector (SE). The composite measurements were performed directly on the metalized surface and cryogenically fractured surface of the samples.

Tensile Tests

The tensile tests were conducted on a EMIC machine, model DL 2000. The stress–strain tests were carried out in accordance with the ASTM D 412 norm using tie beakers type C. The average standard deviation attached to the measurements is lower than 12.5%. This assay was performed on aged samples and nonaged samples, in accordance with ASTM D 573 using a temperature of 70°C for 70 h.
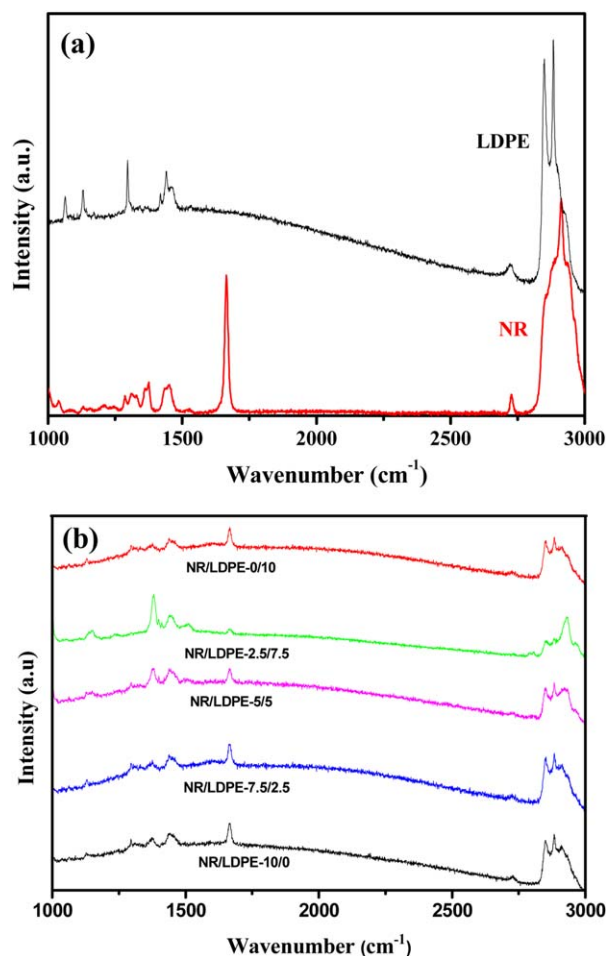

Figure 2. (a) Raman spectra at room temperature of NR and LDPE and (b) of the thermoplastic elastomers NR/LDPE with different proportions of CS and SBA. [Color figure can be viewed in the online issue, which is available at wileyonlinelibrary.com.]
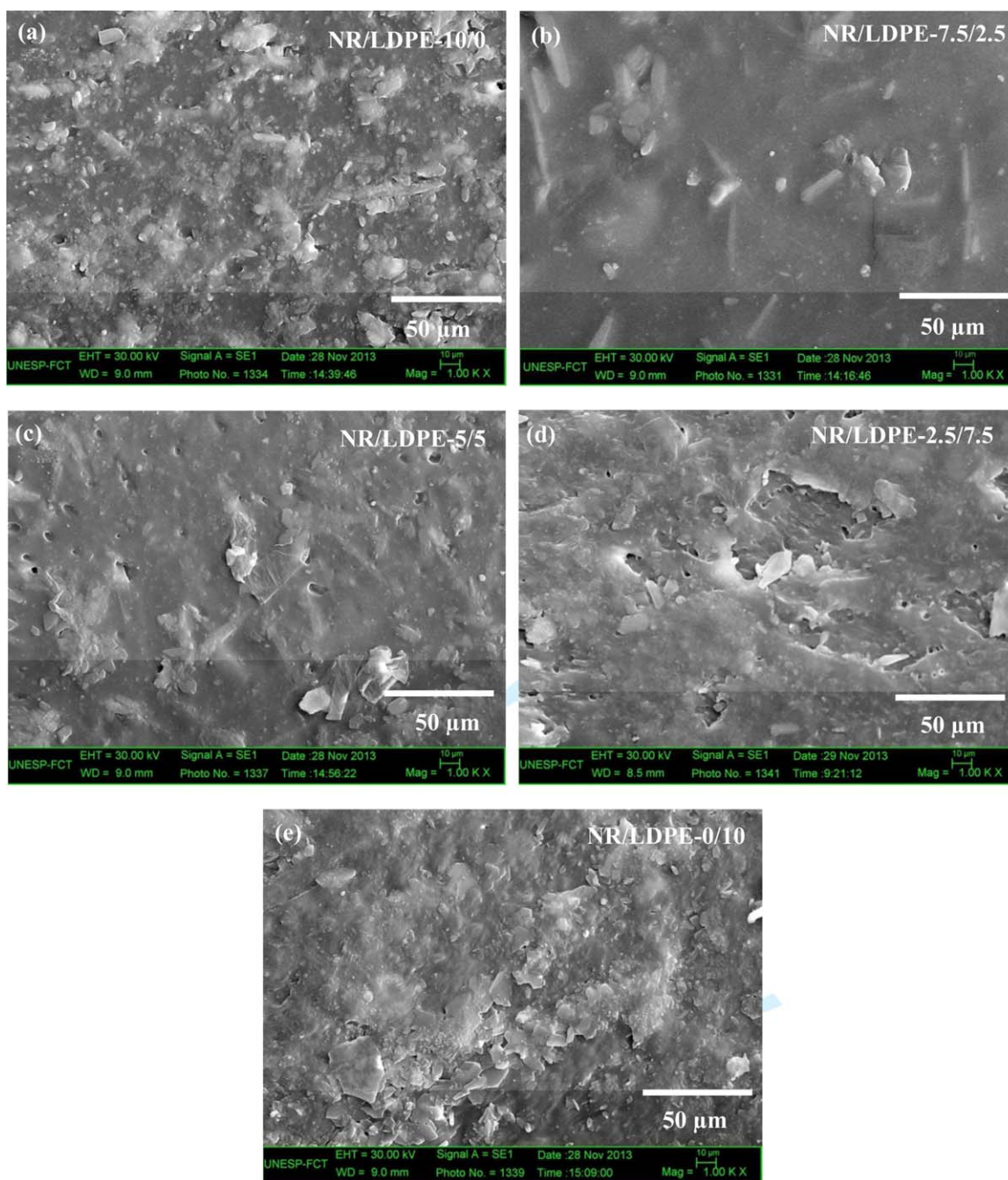
Figure 3. SEM images at room temperature of the surface of (**a**) NR/LDPE-10/0, (**b**) NR/LDPE-7.5/2.5, (**c**) NR/LDPE-5/5, (**d**) NR/LDPE-2.5/7.5, and (**e**) NR/LDPE-0/10 (e) thermoplastic elastomers with magnification equal to 1,000 times. [Color figure can be viewed in the online issue, which is available at wileyonlinelibrary.com.]

RESULTS AND DISCUSSIONS

Structural Characterization

Spectroscopic techniques, such as the Fourier transform infrared spectroscopy (FTIR) and the Raman Spectroscopy (Raman), are analytical techniques used for identifying specific bonds, elements, structures, and interactions between the constituents in the samples. FTIR and Raman are very common techniques due to the accuracy and quickness of the measurement and the relatively low cost of the equipment. The infrared absorption spectra between 4,000 and 600 cm^{-1} for the NR and LDPE (a) and

for the thermoplastic elastomers NR/LDPE with different proportions of CS and SBA are shown in Figure 1. For the NR, the first band is found to be about 832 cm^{-1} which can be attributed to the vibrations of bending in CH group. The bands between 1,088 and 1,367 cm^{-1} are characteristic bands of functional groups present in the cis-1,4-poly-isoprene. In the region between 971 and 1,261 cm^{-1}, vibration associated to swinging in the CH$_3$ can occur while vibrational modes of twist and wag can occur between 1,261 and 1,373 cm^{-1}. The band at 1,462 cm^{-1} refers to the axial deformation modes of CH$_3$
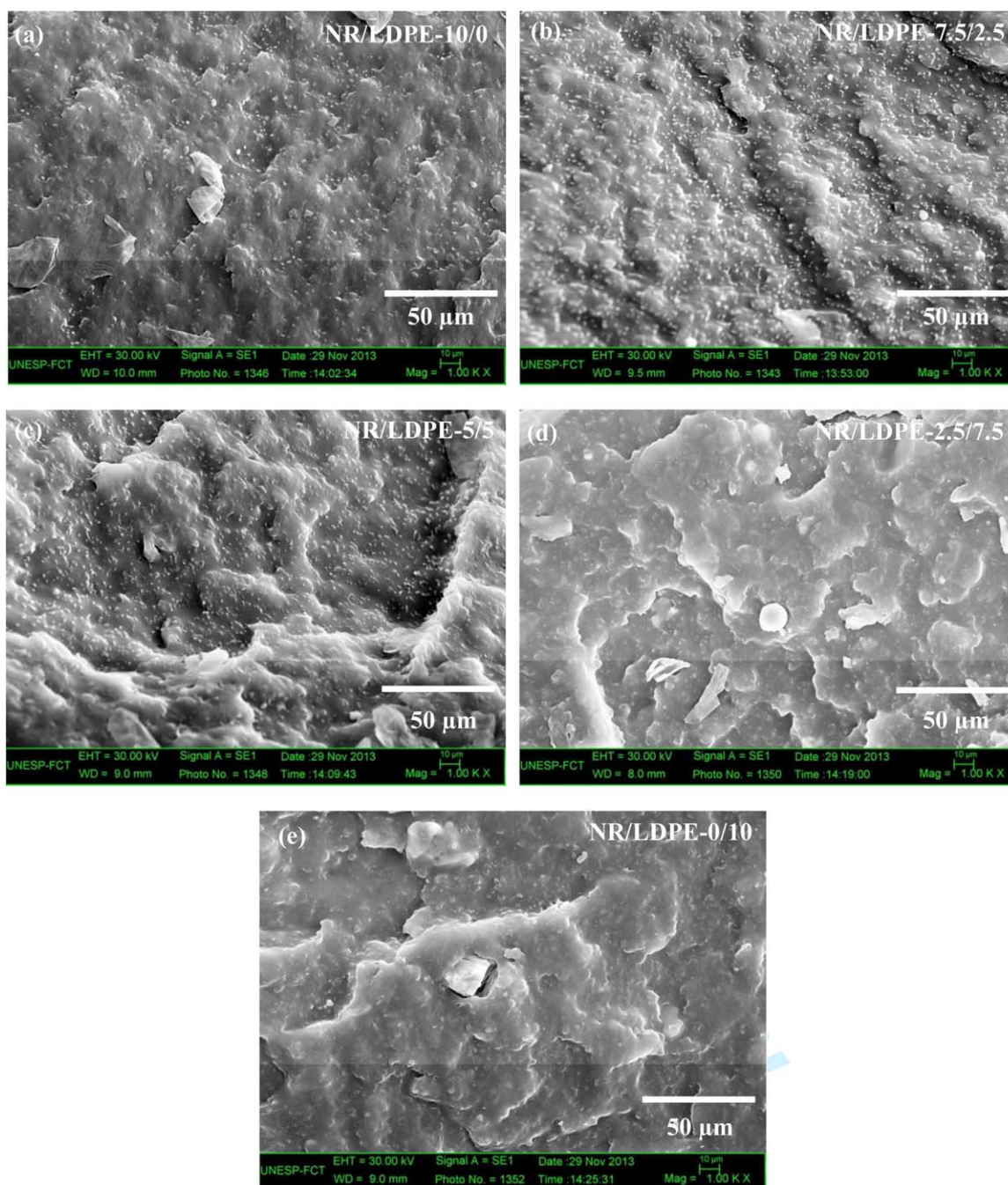
Figure 4. SEM images at room temperature of the cryogenically fractured surface of (**a**) NR/LDPE-10/0, (**b**) NR/LDPE-7.5/2.5, (**c**) NR/LDPE-5/5, (**d**) NR/LDPE-2.5/7.5, and (**e**) NR/LDPE-0/10 thermoplastic elastomers with magnification equal to 1,000 times. [Color figure can be viewed in the online issue, which is available at wileyonlinelibrary.com.]

groups. The bands present between 2,850 and 3,040 cm^{-1} are characteristic of the functional groups of natural rubber while the bands centered in 2,730, 2,850, 2,923, 2,960, and 3,040 cm^{-1} are referred to the symmetric vibrations in CH in CH$_2$ groups, asymmetric vibrations in CH and CH$_2$, asymmetric vibrations of the C-H into the CH$_3$ and stretching mode in =CH.[22] For LDPE, the first band at around 725 cm^{-1} occurs due to the angular bending of CH$_2$ groups. Bands of strong intensity between 971 and 1,373 cm^{-1} were identified and

attributed to the stretching of sulfate groups. The band in 2,850 cm^{-1} corresponds to the symmetric stretching of CH$_2$, the band in 2,960 cm^{-1} is assigned to the asymmetric stretching of CH$_2$. The band of weak intensity in 3,040 cm^{-1} is related to the stretching of OH groups, it is related to atmospheric gases inside the spectrometer chamber. In Figure 1(b), it is possible to see the FTIR spectra of the thermoplastic elastomers NR/LDPE with different proportions of CS and SBA. Note that, regardless of the proportion of CS and SBA, all NR/LDPE
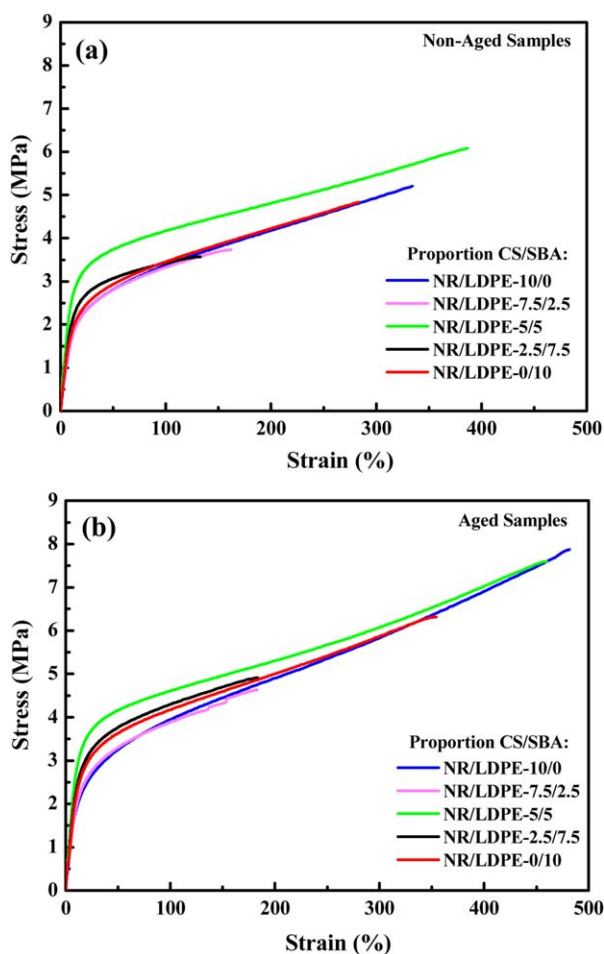
Figure 5. Stress/strain curves between 0 and 500% for thermoplastic elastomers NR/LDPE (a) nonaged and (b) aged with different proportion of CB and SBA. [Color figure can be viewed in the online issue, which is available at wileyonlinelibrary.com.]

spectra show great similarity in comparison with NR and LDPE spectra. In this sense, this observation suggests that there is no chemical interaction between NR and LDPE, only physical interaction, in which NR behaves only as polymeric matrix.

Figure 2 shows the Raman spectra at room temperature of NR and LDPE (a) as well as the Raman spectra of the thermoplastic elastomers NR/LDPE with different proportions of CS and SBA (b). For the LDPE, it is possible to identify a variation in the Raman displacement of the peaks in the low frequency region, $1,000–1,500 \text{ cm}^{-1}$. This region presents vibration modes characteristics of the C–C covalent bonds, indicating that these bonds were distorted in the polymeric chain. For high frequencies, $2,500–3,000 \text{ cm}^{-1}$, alterations in the Raman displacement of the peaks were not observed. The Raman peaks in this region are attributed to the vibration modes of the CH_2 bonds.[23] For the NR, the chain vibration are assigned to C=C, in the "*cis*" part of the rubber chain and they can be seen at around $1,600 \text{ cm}^{-1}$. The vibration modes between 2,700 and $3,000 \text{ cm}^{-1}$ correspond to the stretching of CH groups, in specific CH_2 and CH_3 groups. For the Raman spectra of the thermoplastic elastomers

NR/LDPE, new bands or alterations in the characteristic bands of the NR and LDPE owing to the insertion of CS, SBA, or interaction between matrix and fillers were not observed. As seen in the FTIR spectra, this observation suggests that there is no chemical interaction between NR, LDPE, CS, or SBA.

Morphological Characterization

The scanning electron microscopy (SEM) is an excellent tool to reveal information, for example, superficial and volumetric morphologies and homogeneities, anisotropies, and textures of the samples due to its high magnification and resolution. SEM images at room temperature of the metalized surface and cryogenically fractured surface with magnification of 1,000 times of NR/LDPE-10/0 (a), NR/LDPE-7.5/2.5 (b), NR/LDPE-5/5 (c), NR/LDPE-2.5/7.5 (d), and NR/LDPE-0/10 (e) are shown in Figures 3 and 4, respectively. As can be seen in Figures 3 and 4, a satisfactory superficial cohesion was observed which indicates an efficient mixing process and its appropriate quantities, types of accelerators, conditions for preparing thermoplastic elastomers and satisfactory compatibility between NR, LDPE, CS, and SBA. This satisfactory compatibility can be attributed principally to the large quantity of superficial charges and reactivity of the CB and SBA. For all images, it is possible to observe a low superficial homogeneity with troughs and crests associated with the thermal compression process, the outcrop of components of the vulcanization system, the retention of gases between the sample surface and compression plates and the partial immiscibility between both polymers of the matrix. In terms of superficial homogeneity, the NR/LDPE-7.5/2.5 [Figure 3(b)] was the thermoplastic polymer with better homogeneity probably because this proportion exhibits better conditions for mixing. A special emphasis should be given to the NR/LDPE-0/10 [Figure 3(e)] sample that exhibited a satisfactory surface homogeneity with the replacement of the entire load of CS by SBA representing an ideal condition for waste disposal of sugarcane bagasse.

Table III. Values of Stress and Strain for the Nonaged and Aged Composites, Respectively, with Different Proportion of CS and SBA

Composites	Stress–strain test	
	ε_{MAX} (%)	σ_{MAX} (MPa)
Nonaged samples		
NR/LDPE-10/0	333.7	5.2
NR/LDPE-7.5/2.5	160.8	3.8
NR/LDPE-5.0/5.0	386.5	6.1
NR/LDPE-2.5/7.5	133.9	3.6
NR/LDPE-0/10	282.8	4.9
Aged samples		
NR/LDPE-10/0	443.3	8.0
NR/LDPE-7.5/2.5	183.8	4.6
NR/LDPE-5.0/5.0	466.9	7.9
NR/LDPE-2.5/7.5	182.7	4.9
NR/LDPE-0/10	353.0	6.3

Mechanical Characterization

Mechanical tests, in particular stress/strain tests, are the main source of the technical parameters to determine the quality of a composite material. Assays that include simulations of aging are very relevant for estimating the mechanical performance of the material in the medium and long term. Figure 5 shows the results of mechanical tests in the stress/strain mode between 0% and 500% for thermoplastic polymers NR/LDPE nonaged (a) and aged (b), respectively, with a different proportion of CS and SBA. As can be seen, the stress–strain curves shown in both classes of NR/LDPE (nonaged and aged) are typical for elastomeric materials, indicating that the insertion of charges in these quantities does not alter the overall characteristics of the materials. It is possible to note that there is approximately no difference for the stress (MPa) and deformation (%) in the breaking point independently of the kind of filler used (CS or SBA) or non-aged or aged samples. It should be noted that the materials are not strained to breaking point in normal applications and the lowering of breaking stress does not undermine the material in comparison to the enhancement in elastic properties.

Table III lists the values of stress and strain for the nonaged and aged composites, respectively, with different proportions of CS and SBA. Out of all the samples investigated, NR/LDPE-5/5 showed the best mechanical parameters probably due to dispersion effects or the better vulcanization of the sample. Comparing the mechanical parameters obtained for nonaged and aged samples, the aged samples exhibited better performance probably due to a residual vulcanization process. As required, from a mechanical point of view, the utilization of SBA instead of CS did not cause a significant mechanical alteration in the thermoplastic elastomers which is an indication that the SBA could replace the CS in polymeric materials.

CONCLUSIONS

According to the mechanical results, it appears that the Sugarcane Bagasse Ash (SBA) can be used as a reinforcing filler instead of commercial silica (CS) in thermoplastic elastomers, since there were no significant changes in the mechanical properties of the composite containing CS (NR/LDPE-10/0) in respect to the composite containing SBA (NR/LDPE-0/10). The proportion CS/SBA that had the best mechanical properties was NR/LDPE-5/5. This result is consistent with the morphological analysis, as this same proportion showed better load-matrix interaction. From FTIR and Raman spectroscopes, the prevalence of the characteristic peaks of NR and LDPE was observed in the composite spectra, which comes to confirm that no chemical interaction occurs in the production of composites. In this way, the results point to the possibility of replacing the commercial silica (CS) by sugarcane bagasse ash (SBA) in thermoplastic elastomers produced by NR and LDPE. In addition, this new kind of material is an excellent option for allocation to SBA, contributing to reducing its environmental impact and opening up new economic possibilities for the sugarcane industries.

REFERENCES

1. Gibson, R. F. Principles of Composite Material Mechanics; CRC Press: Boca Raton, **2012**.

2. Mark, J. E.; Erman, B.; Eirich, F. R. Science and Technology of Rubber, 3rd ed.; Elsevier Inc.: Amsterdam, **2005**.

3. Callister, W. D. Jr. Materials Science and Engineering: An Introduction; John Wiley & Sons Inc.: New York, **2000**.

4. Gibson, A. G. Comprehensive Composite Materials: Design and Applications; Elsevier: England, **2000**; Vol. 6, Chapter 6.23: Composite material in the offshore industry.

5. Rattanasom, N.; Saowapark, T.; Deeprasertkul, C. *Polym. Test.* **2007**, *26*, 369.

6. Besco, S.; Brisotto, M.; Gianoncelli, A.; Depero, L. E.; Bontempi, E.; Lorenzetti, A.; Modesti, M. *J. Appl. Polym. Sci.* **2013**, *130*, 4157.

7. Al-Oqla, F. M.; Sapuan, S. M. *J. Clean Prod.* **2014**, *66*, 347.

8. Pires, A.; Martinho, G.; Chang, N. B. *J. Environ. Manage.* **2011**, *92*, 1033.

9. National Supply Company (CONAB) Followup of the Brazilian Cane Sugar 2013/14 - Second Survey, Agosto/2013.

10. Teixeira, S. R.; Peña, A. F. V.; Miguel, A. G. *Waste Manage.* **2010**, *30*, 804.

11. Teixeira, S. R.; Souza, A. E.; Santos, G. T. A.; Peña, A. F. V. *J. Am. Ceram. Soc.* **2008**, *91*, 883.

12. Sales, A.; Lima, S. A. *Waste Manage.* **2010**, *30*, 1114.

13. Rodrigues, C. S.; Ghavami, K.; Stroeven, P. *J. Mater. Sci.* **2006**, *41*, 6925.

14. Kanking, S.; Niltui, P.; Wimolmala, E.; Sombatsompop, N. *Mater. Des.* **2012**, *41*, 74.

15. Cordeiro, G. C.; Toledo Filho, R. D.; Fairbairn, E. M. R.; Tavares, L. M. M. *Cem. Concr. Compos.* **2008**, *30*, 410.

16. Legge, N. R. *Rubber Chem. Technol.* **1987**, *60*, 83.

17. Fiorio, R.; Pistor, V.; Zattera, A. J.; Petzhold, C. L. *Polym. Eng. Sci.* **2012**, *52*, 1678.

18. Jha, K. C.; Tsige, M. *Rubber Chem. Technol.* **2013**, *86*, 401.

19. Tarantili, P. A. *Adv. Elastom. II.* **2013**, *12*, 109.

20. El-Nashar, D. E.; Mansour, S. H.; Girgis, E. *J. Mater. Sci.* **2006**, *41*, 5359.

21. Bellucci, F. S.; Salmazo, L. O.; Budemberg, E. R.; da Silva, M. R.; Rodriguez-Perez, M. A.; Nobre, M. A. L.; Job, A. E. *J. Nanosci. Nanotechnol.* **2012**, *12*, 2691.

22. Chaikumpollert, O.; Sae-Heng, K.; Wakisaka, O.; Mase, A.; Yamamoto, Y.; Kawahara, S. *Polym. Degrad. Stab.* **2011**, *96*, 1989.

23. Tzounis, L.; Debnath, S.; Rooj, S.; Fischer, D.; Mäder, E.; Das, A.; Stamm, M.; Heinrich, G. *Mater. Des.* **2014**, *58*, 1.